

THE QUEST FOR THE TRUE RESIDUAL GAS SATURATION – AN EXPERIMENTAL APPROACH

Øyvind Bull¹, Fred Bratteli², Jon Knut Ringen¹, Karen Melhuus¹, Ann Lisbeth Bye¹,
Jan Erik Iversen²

¹Statoil ASA, ²International Research Institute of Stavanger (IRIS)

This paper was prepared for presentation at the International Symposium of the Society of Core Analysts held in Austin, Texas, USA 18-21 September, 2011

ABSTRACT

Residual gas saturation after water influx is a critical parameter in lean gas reservoirs with strong aquifer support. The mechanism is identified in reservoirs currently subject for field development offshore Norway, and the observed laboratory variations in residual gas saturation constitutes one of the main uncertainties in recoverable reserves.

The majority of publications regarding experimental data focus on identifying correlations of residual gas to petrophysical parameters; initial water saturation, permeability, porosity. While many correlations have represented individual data set with good consistency, few have proven to be valid for sandstone reservoirs in general. Less emphasis has been made on evaluating the experimental techniques being used, and the associated uncertainties. Our experience is that the choice of laboratory method can have a large effect on the residual gas results.

In this paper we present systematic deviations in residual gas saturation depending on the experimental approach. *In situ* saturation monitoring by CT-scanner enable us to study variations in saturation profiles and trapping mechanisms:

- Porous plate imbibition
- Unsteady-state water flood
- Immersed spontaneous imbibition
- CT-observation of porous plate and unsteady-state imbibition
- Pore-network modelling of gas-water displacement

Coreflood simulations are presented to contribute to the discussion of the most representative method for determining the “true” residual gas saturation.

INTRODUCTION

The ultimate recovery in a dry gas reservoir with water drive is largely depending on three factors: i) the residual gas saturation after water flooding, S_{grw} , ii) the corresponding relative permeability to water, $K_{rw}(S_{grw})$, and iii) the remobilization of residual gas during depressurization. In this paper we will focus on data from fields with

strong aquifer influx, where remaining gas saturation after water flooding at constant pressure is a key parameter.

The quest for the true residual gas saturation has been ongoing for decades, yet overshadowed by the holy grail of core analysis, residual oil. Nevertheless, publications reveal a complexity to this parameter that still raises many questions, and we will try to summarize important observations from the literature.

Early research by pioneers on the topic resulted in a basis for common understanding, most of which are still valid today:

- Residual gas measurements in the lab are not sensitive to pressure and temperature conditions or water flooding rate. Simple lab tests at ambient conditions are believed to give reliable data [1-3].
- There is a dependency between initial and residual gas saturation [2,4], captured by the widely recognized Land correlation [5].
- There is an overall correlation between residual gas and porosity, but no common trend with other petrophysical parameters [2,3,6,7].

A great effort has been made to find robust correlations of S_{grw} with other rock properties. A weak trend with microporosity has been identified [8-10], generally explained by a low pore body-to-throat aspect ratio in micropores, causing little or no trapping of gas. Accordingly, Jerauld [8] concluded that grain size was more effective than porosity for correlating trapped gas. The impact of matrix boundary conditions during counter-current imbibition and scaling challenges has been clearly pointed out [11,12]. Furthermore, there has been much focus on empirical equations that better represent the experimental data [5,8,9,13-16]. While many correlations have represented individual data set with good consistency, few have proven to be valid for sandstone or carbonate reservoirs in general.

Acknowledging the importance of this research, we will concentrate on the impact of experimental methods, conditions and related uncertainties. Available published data is limited, which is comprehensible given the early on disregard of laboratory methodology. Several authors have supported this assumption, observing that neither flow rate [1-3,18,19], pore pressure [1,2,18], wetting liquid [1,8,10,20], temperature [2,18] nor experimental method [1,3,10,17] affect the total S_{grw} . But there are also contradictions in the reported data.

Babadagli *et al.* [12] reported an increase in gas recovery with increasing temperature, attributed to reduction in surface tension and water viscosities. Mulyadi *et al.* [20] compared four experimental methods: steady-state, co-current, counter-current and centrifuge imbibition. Despite limited data, the measured residual gas saturation systematically differed with experimental method, and submerged counter-current imbibition at ambient condition yielded in average 7% lower S_{grw} compared to co-current imbibition performed with pore pressure. Geffen *et al.* [1] reported no effect of

flooding rate or pore pressure, but by changing more than one parameter in each step the background data become somewhat inconclusive.

The effect of diffusion is discussed by many authors, but there is only sparse documentation of its relative contribution to Sgrw at ambient conditions [21]. When evaluating data from immersed spontaneous imbibition, the production profile vs. square root of time is often characterized by rapid initial imbibition (Pc dominated) followed by a tail production (diffusion dominated). Sgrw is typically defined at the intersection between these two trends [10]. All experiments performed at atmospheric pressure must correct for diffusion, which introduces an additional uncertainty to the results. The transition from capillary to diffusion dominated recovery is not always sharply defined, meaning that these mechanisms are overlapping, and the relative contributions are not obvious. By comparison, water-oil imbibition in water-wet sandstone also shows a certain degree of tail production [11], but diffusion effects are absent. The diffusion will start acting behind the water front, where trapped gas will re-equilibrate with the surrounding water due to “local” capillary pressure. We can estimate this capillary pressure using a simplified Laplace’s equation:

$$P_c = 2 * \sigma * \cos(\varphi)/r \quad (1)$$

where σ is the gas-water interfacial tension, φ the contact angle and r the pore throat radius. If we consider gas trapped in a water-wet sandstone pore: 10 micron pore throat radius, $\sigma = 72$ dynes/cm and $\varphi=0$, the capillary forces will act with 0.14 bar pressure. Hence an imbibition experiment at atmospheric conditions may experience a relative compression of the residual gas by 10-20%. These effects are important and will be even more significant for tighter systems. Diffusion gas will migrate through the continuous water phase, connecting to mobile gas and be produced. Jerauld [8] propose diffusion as an explanation to the apparent absence of gas trapping in micropores, and assumes the effect will be similar at reservoir conditions. However, we will argue that compression and diffusion effects will be limited or absent at reservoir conditions, where the relative pressure change is much smaller.

We suspect that the general scatter in published data on residual gas is not only attributed to rock properties, but also to the design and conditions of the experiment.

Material and Methods

Core material

The presented results are originating mainly from two sandstone formations on the Norwegian Continental Shelf, from field A and B, where an extensive experimental program has been ongoing throughout the last year. A characterization is given below:

- **Field A:** Medium-to-fine grain size, moderate-to-poor consolidation and an average content of 85wt% quartz and 3wt% clays, mainly kaolinite and illite. Typical permeability range 200 mD-3 D, porosity range 0.25-0.34.
- **Field B:** Medium-to-very-fine grain size, well consolidated and an average content of 82wt% quartz and 6wt% clays, mainly kaolinite and illite. Typical permeability range 10-500 mD, porosity range 0.21-0.28.

From mercury injection experiments, both formations show a slight bimodal pore size distribution, but are dominated by pore throat radii from 5-10 μ m. Plug dimension is 1.5” diameter and 6-8cm length, and all samples were run through a CT-scanner to verify good quality and preserved integrity. For a broader comparison, we will also present general trends from several other North Sea sandstone gas reservoirs.

Preparation of core material

Initially, the core plugs were cleaned at 20 bar net confining stress in a core holder by flooding toluene and methanol at 70°C. After miscible displacement with simulated formation water at ambient temperature, absolute water permeability was determined.

Semi permeable ceramic porous plates were installed at the outlet of each core plug. To maintain hydraulic contact between plug surface and porous plate, kaolinite paste was applied. Then the core plugs were drained to irreducible water saturation, S_{wi} , with humidified nitrogen gas. Drainage pressure was increased gradually to 15 bar, allowing a maximum gas rate of 1 cc/day to limit any effect from viscous forces. Typical drainage time was 6 to 8 weeks. With one exception, each plug was only used for one experiment.

Porous plate imbibition

At S_{wi} , outlet pressure was raised to 20 bar simultaneously with an increase of pore pressure to 35 bar. The capillary pressure of 15 bar was maintained during this process. Subsequently, pore pressure was reduced gradually to 20 bar, *i.e.* $P_c=0$ bar. This was to allow a spontaneous imbibition of gas-equilibrated water. Typically, this process ceased within 6 to 8 weeks. Imbibed volumes were recorded from readings of water level in glass burette and checked with saturation control using Karl Fischer titration. A schematic diagram over the experimental setup is shown in Figure 1A.

Unsteady-state water flood (USS)

At S_{wi} , gas permeability, $K_g(S_{wi})$ was measured. The pore pressure was raised to 20 bar, and gas-water equilibrium was maintained. The plugs were then flooded with simulated formation water at a flow rate of 4 cc/hr until steady-state conditions prevailed. Permeability to water at residual gas saturation, $K_w(S_{grw})$, was measured. The residual gas saturation was determined from the collected gas volume and checked with Karl Fischer titration. Experimental setup is shown in Figure 1B.

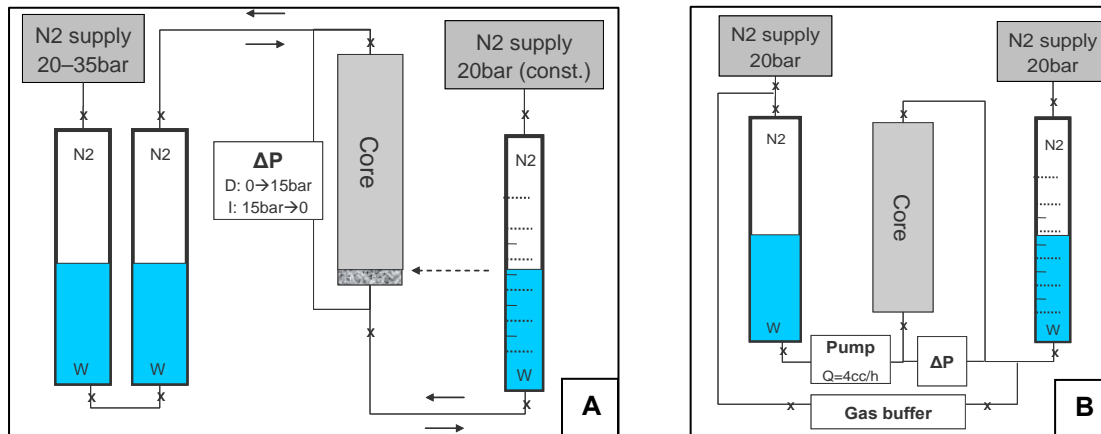


Figure 1: Schematic diagram for A) Porous plate imbibition and B) Unsteady-state experimental setup.

Immersed spontaneous imbibition

Water imbibition was performed by immersing the lower part of the plug on to the surface of a water bath and measure weight change over time. The sample was suspended from a hook underneath a balance. To secure a one dimensional imbibition, the plug was confined with shrinkable Teflon tubing. At constant weight, typically after 1 hour, the plug was lowered to a position so that the upper end face was at water level, *i.e.* fully immersed. Weights were recorded until constant. The procedure was repeated with a dummy plug of plastic to account for evaporation, and buoyancy loss due to imbibed water was corrected for. Schematics of the experimental setup are presented in Hamon *et al.* [10].

CT-observation of porous plate imbibition and unsteady-state water flooding

The objective of the CT measurements was to repeat the porous plate and USS experiments, while obtaining high resolution *in situ* saturation profiles. The experimental procedure is principally similar, with the one exception that the CT-rig was limited to a horizontal core holder position.

Pore-network modelling of water-gas displacement

Pore scale modelling was performed by Numerical Rocks as an alternative independent method for estimating residual gas saturation. Rock models of 3 samples from field A were reconstructed based on backscattered electron microscope (BSEM) images of thin sections. Three model realizations were reconstructed per sample in order to capture heterogeneities observed in the thin section. The models were quality checked visually and statistically against thin section images, and petrophysical properties calculated. From extracted pore networks, fluid flow was simulated, using a gas-water interfacial tension of 70 dynes/cm and water wet advancing contact angles from 20-60°. The reported data are limited to residual gas saturation, S_{grw} , and the corresponding end point relative permeability to water, $K_{rw}(S_{grw})$.

RESULTS

Table 1 and 2 summarizes the key results from our residual gas evaluation. The core based experiments have been performed at three independent laboratories, and show a consistent agreement in data.

Porous plate imbibition and unsteady-state water flooding

Residual gas saturation from porous plate imbibition and unsteady-state water flooding constitutes our main basis for data evaluation, and is compared in Figure 2 versus porosity and irreducible water saturation. We see a systematic difference in S_{grw} depending on the experimental method of approach; with porous plate imbibition yielding an average of 14% lower residual gas saturation. In Figure 3 we have included other available data from North Sea sandstone reservoirs, suggesting that the trend observed for Field A and B is representative for a variety of rock properties.

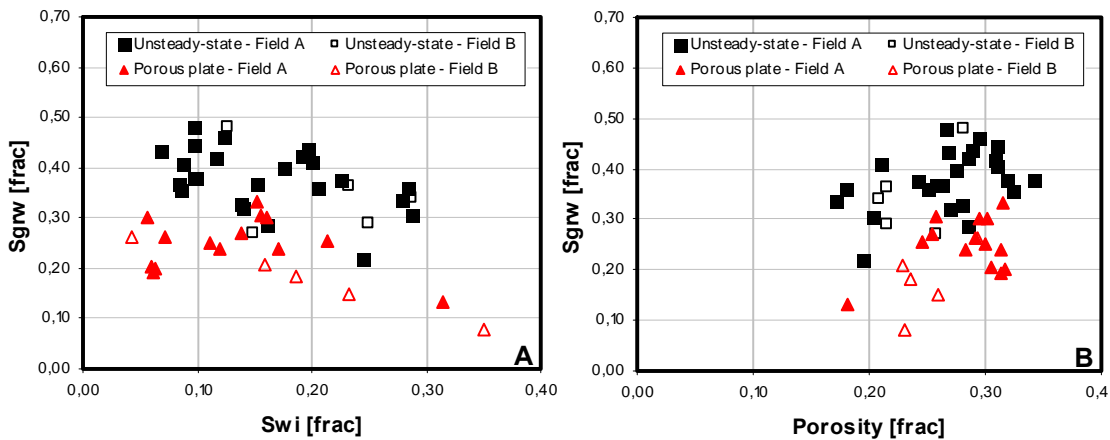


Figure 2: Residual gas saturation vs. A) initial water saturation and B) porosity.

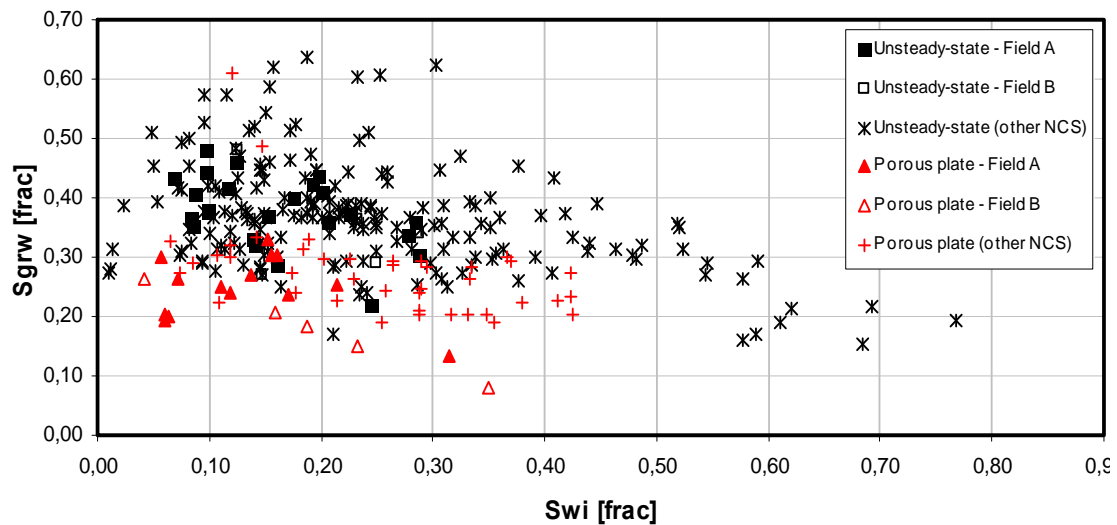


Figure 3: Residual gas saturation vs. initial water saturation, Field A and B compared to other NCS data.

Immersed spontaneous imbibition

Figure 4 shows the increase in water saturation versus the square root of time during immersed spontaneous imbibition, measured on core material from Field A. The residual gas saturation reported in Table 2 is based on the intersection between curve trends before and after the distinct decrease in imbibition rate. Traditionally the first part of the curve has been regarded as a capillary dominated, whereas the secondary part is diffusion dominated [10]. As can be seen from Figure 4, there is a significant increase in water saturation at a later time, corresponding to the samples being fully submerged in brine. Whether this contribution is attributed to capillary pressure or diffusion is yet to be defined.

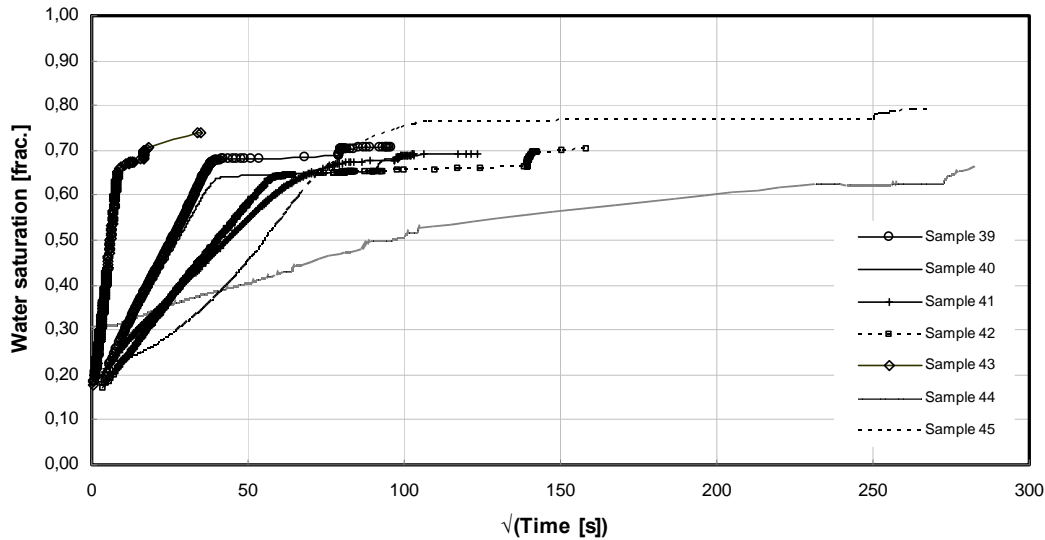


Figure 4: Water saturation vs. square root of imbibition time.

CT-observation of porous plate imbibition and unsteady-state water flooding

To further investigate the observed difference in S_{grw} between porous plate imbibition and USS water flooding, we repeated the experiments using a CT scanner for *in situ* saturation monitoring. The final results are reported in Table 1-2.

Figure 5A shows a CT snap-shot and successive saturation profiles during porous plate drainage on a Field B plug, indicating a stable desaturation process with no end-effects. The slight bump in the middle part of the plug is related to lower porosity, identified from CT density mapping. The subsequent slow imbibition process, by a controlled P_c reduction to $P_c=0$, is presented in Figure 5B. The displacement front is dispersed along the entire plug length, resulting in a nearly uniform increase in water saturation. The final residual gas saturation, however, is significantly higher than previously measured on the same plug. We suspect that this is an experimental artefact, possibly caused by lack of a sufficient capillary contact between plate and plug.

The saturation profiles during USS water flooding at 4 cc/h are presented in Figure 5C. Despite the horizontal orientation of the plug in the CT-rig, no segregation was observed,

but rather a sharp displacement front. After breakthrough at 0.36 PV injected, no further gas was produced, which is expected for a strongly water-wet system. The same observation was made during all the USS experiments.

Pore-network modelling of gas-water displacement

Results from the pore-network modelling on field A samples are reported in Table 2. The residual gas saturation ranges from between 0.27 and 0.37, and lies between the observed trends for USS and porous plate experiments. End point relative permeability to water, however, is almost an order of magnitude higher than the lab based measurements, which question the validity for meaningful comparison. This will be further discussed below.

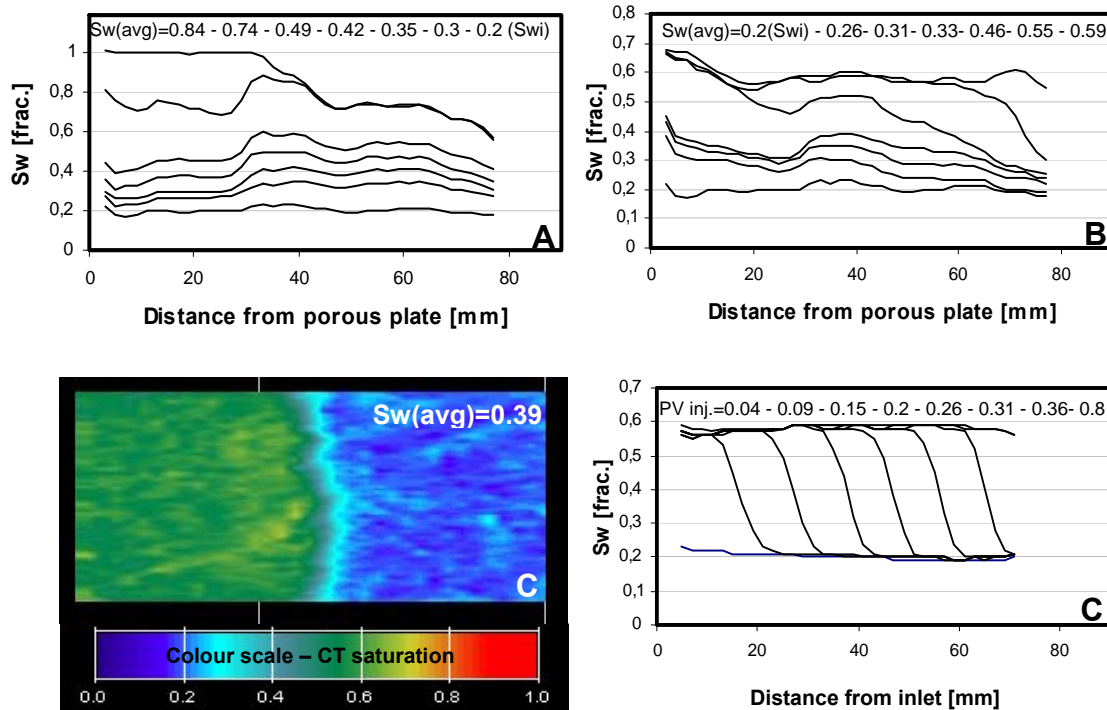


Figure 5: CT snap-shots and successive saturation profiles during A) Porous plate drainage, B) Porous plate imbibition and C) Unsteady-state imbibition.

Discussion

Effect of flow rate on residual gas saturation

Our results show a clear connection between water imbibition rate and residual gas saturation, an effect that has been regarded insignificant by several authors [1-3,18,19]. But while previous conclusions have been based on more or less single plug comparisons, we present herein a larger dataset indicating a systematic shift in S_{grw} with imbibition rate on various reservoir sandstones.

Reproducing the USS and porous plate experiments in a CT-rig revealed a significant variation in the displacement front. Water flooding at 4 cc/h produced a piston like

displacement, even though the flow rate seems to be below the free spontaneous imbibition rate. Several observations support this assumption:

- Negative differential pressure until water breakthrough
- No gas production after water breakthrough in USS experiments
- The immersed spontaneous imbibition terminated after about 1 hour. The unsteady state breakthrough time was typically 2 hours with similar initial and residual saturations.

Saturation profiles imaged during porous plate imbibition show a dispersed displacement front across the entire plug. This process is also governed by capillary forces alone, but with a much lower rate controlled by the permeability of the ceramic plate. A similar rate dependent saturation profile was observed by Geffen *et al.* [1] and Delclaud [18]. They concluded with no important rate effects as the final residual gas saturation was similar, but as previously discussed, we find the data basis somewhat questionable.

From the observations made in our studies, we suspect a rate dependent shift in the gas trapping mechanism. Kumar *et al.* [22] used micro-CT imaging to visualize the fluid distribution in the pore space after counter-current imbibition, and identified that the gas phase was generally trapped in large clusters, most spanning over multiple pore lengths. Ding *et al.* [17] concluded that counter-current imbibition in water-wet samples gave a piston displacement, where gas was trapped in smaller and larger pores simultaneously. Building on these statements with our own observations, we put forward a hypothesis explaining the effect of imbibition rate on residual gas saturation.

- At a sufficiently low imbibition rate, capillary forces will lead to gas trapping in the smallest pores first, then in subsequently larger and more conductive pores as more water becomes “available”. The results will be a dispersed displacement front, as identified in our porous plate CT-experiment.
- In the opposite case, a sharp displacement front will cause gas trapping in smaller and larger pores simultaneously. Gas trapped in larger pores or pore clusters, could potentially restrict gas from escaping from smaller neighbouring pores, if the conductive pathway has been blocked.

This will make the front velocity in the reservoir an important parameter when estimating the residual gas saturation. The front velocity in the USS experiments was around 1 m/day; in the same range as for the immersed imbibition experiments. During porous plate imbibition, the front velocity was around 3 m/year.

Effect of pore pressure on residual gas saturation

The immersed spontaneous imbibition data was obtained for reference, as this technique is most commonly seen in the residual gas literature. The data fall between the porous plate and unsteady-state results, but the pore pressures are different. Knowing that gas is highly compressible and subject to diffusion, we believe that applying an elevated or

reservoir pore pressure will decrease these contributions considerably. The two-step imbibition profile in Figure 4 emphasizes that ambient effect corrections can be complex, and may increase the uncertainty in reported data. Several authors have pointed out that microporosity tends not to trap gas [8-10], but the related dependency of pore pressure has not been investigated. Dacy [23] observes low residual gas from counter-current imbibition in dry plugs from (microporous) tight gas sand formations, and attributes this to diffusion effects. While a typical Land-correlation show a flat trend at high initial gas saturation, Suzanne *et al.* [9] show an almost linear trend for Fontainebleau sandstone, which is almost free of clays (and microporosity). We suspect that the reservoir pore pressure would act to straighten this curve by reducing diffusion effects.

PNM simulations

The mismatch between PNM and experimental $K_{rw}(S_{grw})$ -results is not fully understood. The main experimental uncertainty is a low pressure drop at S_{grw} , however there is a good consistency in the data over a wide permeability range. A recent study [24] concluded that the PNM simulator required unrealistic contact angles to obtain reasonable S_{grw} -data. Because of this, however, the simulator has been updated to honour tortuosity, topology and pore geometry explicitly in the calculations. We do not have sufficient statistics to conclude in this matter.

Coreflood simulations

Coreflood simulations (Sendra) were performed to verify that the observed rate dependency on displacement front was a physical effect. The models were designed to capture the plug properties of the CT-samples. Water-gas USS relative permeability and imbibition porous plate capillary pressure were adopted from analogue samples within the same formation. Figure 6A shows the saturation profile at 0.3 pore volumes injected water, and at four different flow rates. The simulated data confirm a clear non-linear rate dependency, but the ultimate recovery is similar. In Figure 6B we compare the simulated and experimental saturation profiles during USS and porous plate imbibition, where the latter was modelled as an USS experiment with very low flow rate (estimated). There is a good agreement between experiment and simulation.

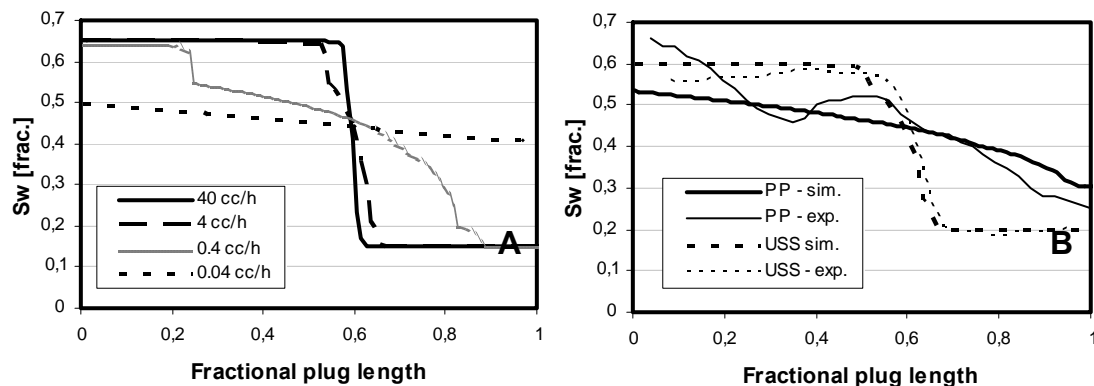


Figure 6: A) Simulated saturation profiles at 0.3 PV injected, B) Comparison of simulated and experimental results.

CONCLUSIONS

- Residual gas saturation in water-wet sandstones is dependent on imbibition rate. Low rate USS water flooding and immersed imbibition show significantly higher Sgrw than ultra slow imbibition controlled by porous plate.
- CT-scanning has revealed a dispersed water front at very low imbibition rates, while rates similar to the free spontaneous imbibition results in a piston like displacement. The data has been verified by coreflood simulations.
- Based on the Sgrw data and CT-imaging, we suspect that the variation in Sgrw is related to the shape of the displacement front, where a dispersed profile leads to less trapping of gas.
- We believe that residual gas measurements should be performed at elevated or reservoir pore pressure, to limit any effect of gas compression and diffusion.

ACKNOWLEDGEMENTS

The authors would like to thank Numerical Rocks and Weatherford Laboratories Norway for important data contributions. We would also like to thank Statoil ASA for permission to publish the SCAL data presented in this paper.

Table 1: USS imbibition data.

Field	Sample ID	Porosity [frac]	Klink. corr. perm [mD]	Swi [frac]	Sgrw [frac]	Krw(Sgrw) [frac]
A	1	0,31	2145	0,10	0,45	0,008
	2	0,32	2450	0,09	0,35	0,012
	3	0,26	3234	0,08	0,37	0,016
	4	0,32	1734	0,10	0,38	0,033
	5	0,34	2154	0,10	0,38	0,012
	6	0,30	1395	0,12	0,46	0,009
	7	0,28	1092	0,16	0,29	0,015
	8	0,28	1594	0,14	0,33	0,020
	9	0,27	1098	0,18	0,40	0,017
	10	0,29	724	0,19	0,42	0,014
	11	0,29	506	0,20	0,44	0,007
	12	0,20	34,3	0,29	0,30	0,008
	13	0,17	30,2	0,28	0,34	0,009
	14	0,20	51,2	0,24	0,22	0,007
	15	0,27	221	0,10	0,48	0,010
	16	0,26	329	0,15	0,37	0,011
	17	0,25	462	0,21	0,36	0,009
	18	0,18	195	0,28	0,36	0,020
	19	0,31	1432	0,09	0,41	0,052
	20	0,31	1045	0,12	0,42	0,040
	21	0,27	1172	0,07	0,43	0,027
	22	0,24	315	0,23	0,37	0,013
	23	0,27	535	0,14	0,32	-
24- CT	0,21	56	0,20	0,41	0,025	
B	49	0,26	291	0,15	0,27	0,102
	50	0,22	119	0,25	0,29	0,084
	51	0,28	384	0,13	0,48	0,021
	52	0,22	93	0,23	0,37	0,027
	53	0,21	10,2	0,29	0,34	0,014

Table 2: Other imbibition data

Field	Sample ID	Experiment type	Porosity [frac]	Klink. corr. perm [mD]	Swi [frac]	Sgrw [frac]	Krw(Sgrw) [frac]
A	25	Porous plate	0,30	995	0,11	0,25	-
	26		0,28	429	0,17	0,24	-
	27		0,30	619	0,16	0,30	-
	28		0,32	814	0,15	0,33	-
	29		0,31	535	0,12	0,24	-
	30		0,26	117	0,16	0,31	-
	31		0,30	63,7	0,06	0,30	-
	32		0,25	209	0,14	0,27	-
	33		0,18	9,83	0,32	0,13	-
	34		0,31	1404	0,06	0,21	-
	35		0,31	44,1	0,06	0,19	-
	36		0,32	605	0,06	0,20	-
	37		0,25	335	0,21	0,26	-
	38		0,29	2053	0,07	0,26	-
A	39	Immersed	0,28	448	0,17	0,32	-
	40		0,27	491	0,17	0,36	-
	41		0,27	770	0,18	0,33	-
	42		0,28	273	0,16	0,36	-
	43		0,28	910	0,18	0,34	-
	44		0,24	1052	0,31	0,37	-
A	45	PNM	0,27	721	0,22	0,23	-
	46		0,27	597	0,17	0,37	0,15
A	47	PNM	0,27	613	0,15	0,36	0,19
	48		0,30	3874	0,12	0,27	0,32
B	54	PP	0,29	6516	0,04	0,26	-
	55		0,23	243	0,16	0,21	-
	56		0,24	306	0,19	0,18	-
	57		0,23	2,86	0,35	0,08	-
	58		0,26	91,9	0,23	0,15	-
	58 - CT		0,26	91,9	0,20	0,41	-

REFERENCES

1. Geffen T.M., Parish D.R., Haynes G.W., Morse R.A., "Efficiency of gas displacement from porous media by liquid flooding", *Trans. AIME*, (1952), v **195**, pp 29-38
2. Chierici G.L., Ciucci G.M., Long G., "Experimental research on gas saturation behind the water front in gas reservoirs subjected to water drive", *World Petroleum Congress*, (1963) **sec II-17**, PD6, pp 483-498
3. Mc Kay B.A., "Laboratory studies of gas displacement from sandstone reservoirs having strong water drive", *APEA Journal*, (1974), pp 189-194
4. Land C.S., "Calculation of imbibition relative permeability for two and three phase flow from rock properties"; *SPEJ* (June 1968), v **8**, n 2, pp 149-156
5. Land C.S., "Comparison of calculated with experimental imbibition relative permeability", SPE 3360, (1971)
6. Katz D.L., Legatski M.W., Tek M.W., Gorring M.R., Neilsen R.L., "How water displaces gas from porous media", *Oil and Gas Journal*, (1966), pp 55-60
7. Keelan D.K., Dugh V.J., "Trapped-gas saturation in carbonate formations", SPE 4535, (1975)
8. Jerauld G.R., "Gas-oil relative permeability of Prudhoe bay", *SPE*, SPE 35718, (1997), pp 653-670
9. Suzanne, K., Hamon, G., Billiotte J., Trocm, e.V., "Experimental relationships between residual gas saturation and initial gas saturation in heterogeneous sandstone reservoirs", SPE 84038, (2003)
10. Hamon, G., Suzanne K., Billiotte J., Trocme V., "Field-wide variations of trapped gas saturation in heterogeneous sandstone reservoirs", SPE 71524, (2001)
11. Zhang, X., Morrow, N.R., and Ma, S., "Experimental Verification of a Modified Scaling Group for Spontaneous Imbibition", *SPE*, (1996), p280
12. Babadagli, T., Hatiboglu, C.U., "Gas-Water Counter-Current Capillary Imbibition at Different Temperatures", SPE 93882, (2005)
13. Kantzas, A., Ding, M., and Lee, J., "Residual gas saturation revisited", SPE 59782, (2000)
14. Kleppe, J., Hamon, G. and Chaput, E., "Representation of Capillary Pressure Hysteresis in Reservoir Simulations", SPE 38899, (1997)
15. Ding, M., Kantzas, A., "Measurements of residual gas saturation under ambient conditions", *Proceedings of the Annual Symposium of the Society of Core Analysts*, SCA2001-33, Edinburg, Scotland
16. Spiteri, E.J., Juanes, R., Blunt, M.J., and Orr Jr., F.M., "A New Model of Trapping and Relative Permeability Hysteresis for All Wettability Characteristics", *SPE*, **13** (3): 277-288. SPE 96448-PA, (2008)
17. Ding, M. and Kantzas, A., "Evaluation of gas saturation during water imbibition experiments", CIPC 2003-021 Canadian International Petroleum Conference, Calgary, Alberta Canada June 10-12, (2003)
18. Delclaud J., "Laboratory measurements of the residual gas saturation", *Second European Core Analysis Symposium*, (1987), pp 431-451
19. Crowell D.C., Dean G.W., Loomis A.G., "Efficiency of gas displacement from a water-drive reservoir", *Report of investigations*, 6735 USBM, (1966), pp 1- 29
20. Mulyadi, H., Amin, R., Kennaird, T., Bakker, G., Palmer, I., Van Nispen, D., "Measurement of Residual Gas Saturation in Water-Driven Gas Reservoirs: Comparison of Various Core Analysis Techniques", SPE 64710, (2000)
21. Ding, M., Kantzas, A., "Estimation of residual gas saturation from different reservoirs", PETSOC 2004-061, (2004)
22. Kumar, M., Senden, T.J., Sheppard, A.P., Middleton, J.P., Knackstedt, M.A., "Visualizing and Quantifying the Residual Phase Distribution in Core Material", *Proceedings of the Annual Symposium of the Society of Core Analysts*, SCA2009-16, Noordwijk, Netherlands
23. Dacy, J.M., "Core Tests for Relative Permeability of Unconventional Gas Reservoirs", SPE 135427, (2010)
24. Caubit, C., Hamon, G., Sheppard, A.P. and Øren, P.E., "Evaluation of the reliability of prediction of petrophysical data through imagery and pore network modelling", *Proceedings of the Annual Symposium of the Society of Core Analysts*, SCA2008-33, Abu Dhabi, U.A.E.